

QGP formation and strange antibaryons

Johann Rafelski¹, Jean Letessier² and Ahmed Tounsi²

¹Department of Physics, University of Arizona, Tucson, AZ 85721

²Laboratoire de Physique Théorique et Hautes Energies*

Université Paris 7, 2 place Jussieu, F-75251 Cedex 05.

Published in Phys. Lett B390 (1997) 363

Abstract

We analyze current experimental results and explore, as function of the collision energy and stopping in relativistic nuclear collisions, the production yields of strange antibaryons, assuming formation of a deconfined thermal QGP-fireball which undergoes a sudden hadronisation.

PACS numbers: 25.75.+r, 12.38.Mh, 24.85.+p

We present here a brief account of a study of the hadronic probes of quark-gluon plasma (QGP) involving in particular strange antibaryons. Hadronic particles can probe the QGP phase provided that there is rapid final state disintegration — in this case the abundances and spectra of hadrons reflect the conditions in the QGP [1, 2].

We assume thermalization of initially participating hadronic matter, and the formation in the collision at currently accessible energies $\sqrt{s} \leq 10A$ GeV of a baryon-rich fireball in the central rapidity region. The latter hypothesis is inferred from the observed [3] rapidity distribution of Λ and $\bar{\Lambda}$. These and other results show that the S-Ag/W/Pb and even the S-S collisions up to 200A GeV are very different from the ultra-relativistic limit [4], in which the valence quarks are expected to leave the central rapidity region. Furthermore, the anticipated [5] and experimentally confirmed [3, 6, 7] high production rate of (multiply) strange antibaryons in A-A reactions, and their central (in rapidity) spectral distributions are indicating a collective particle formation mechanism [8]: in the QGP reaction picture it is the ready made high density of (anti) strange quarks which leads under the rapid hadronisation scenario to high yields of (multiply) strange particles[5].

Particle yields from a rapidly dissociating fireball are proportional to the QGP particle fugacities λ_i , $i = u, d, s$: the fugacity of hadronic particles is the product of the valence quark fugacities, e.g. hyperons have the fugacity $\lambda_Y = \lambda_u \lambda_d \lambda_s$. Because of u - d symmetry

*Unité associée au CNRS UA 280.

just one light quark fugacity $\lambda_q^2 \equiv \lambda_d \lambda_u$ will be considered here. One often uses the chemical potentials μ_i : $\lambda_i = e^{\mu_i/T}$. The chemical potentials for particles and antiparticles are opposite to each other, provided that chemical equilibrium has been established: we speak of *relative* chemical equilibrium when particle abundances are in relative equilibrium with each other, and of *absolute* equilibrium when the total particle yields are completely filling the available phase space. Calculations [9, 10] show that strangeness will not always fully saturate the available phase-space. Therefore, we consider the associated off-equilibrium parameter γ_s [1]:

$$\gamma_s(t) \equiv \frac{\int d^3p d^3x n_s(\vec{p}, \vec{x}; t)}{\int d^3p d^3x n_s^\infty(\vec{p}, \vec{x})}, \quad (1)$$

where n_s^∞ is the equilibrium particle density. This definition presupposes that since the thermal equilibrium is established within a shorter time scale than the (absolute) chemical equilibrium, the saturation of the (strangeness) phase space can be described by a momentum independent factor. The above definition applies in analogous fashion to light quarks (γ_q) and gluons (γ_G). It is straightforward to extract from the strange antibaryon experimental particle yields [11] the value of γ_s . The presence of valance quarks in the fireball helps light quarks and gluons to equilibrate during the duration of the nuclear collision, and at $t_{\text{ch}} \simeq 1.5$ fm/c in the CM frame we take $\gamma_q \rightarrow 1$, $\gamma_G \rightarrow 1$, but $\gamma_s \simeq 1/7$, appropriate for a 7 times slower strange quark relaxation time [10].

The specific energy E/B in the fireball is initially only a function of the CM-energy E_{CM} , and the stopping fractions of energy η_E and baryon number η_B :

$$\frac{E}{B} = \frac{\eta_E E_{\text{CM}}}{\eta_B A_{\text{part}}}, \quad (2)$$

where A_{part} is the number of nucleons participating in the reaction. When the projectile is smaller than the target, we have assumed a collision with the geometric target tube of matter. In the case that the stopping fractions are equal $\eta_E \simeq \eta_B$ the resulting specific fireball energies are shown in the heading of the columns in table 1: $2.6 < E/B < 8.8$ GeV. These values correspond to, in turn: Au–Si and Au–Au collisions at AGS, possible future Pb–Pb collisions at SPS with 40A GeV, S–Pb at 200A GeV, and for the Pb–Pb collisions at 158A GeV, we considered two possible values of energy/momentum stopping $\eta = 3/4$ and $\eta = 1$.

A second condition constraining the initial conditions of the fireball arises from the balance between the fireball thermal pressure and the pressure due to kinetic motion:

$$P_{\text{dyn}} = \eta_p \rho_0 p_{\text{CM}}^2 / E_{\text{CM}}. \quad (3)$$

Here a fraction $0 \leq \eta_p \leq 1$ of the incident CM momentum can be used by a particle incident on the central fireball in order to exert dynamical pressure[13]. In the relativistic limit we have $\eta_p \simeq \eta_E \equiv \eta$ since the momentum and energy of a particle are nearly equal when the velocity $v \simeq c$.

Because the QGP phase fireball is initially also strangeness neutral we have $\lambda_s = 1$. Therefore, the above two conditions fix the two open statistical parameters of the fireball T_{ch} and λ_q , shown in the columns of the top section of table 1. Each column also shows other

Table 1: Properties of different collision fireballs.

Phase space occupancy	$\langle s - \bar{s} \rangle = 0$ $\lambda_s \equiv 1$	E/B [GeV]				
		2.6 $\eta = 1$ Au–Au	4.3 $\eta = 1$ Pb–Pb	8.8 $\eta = 0.5$ S–Pb	8.6 $\eta = 0.75$ Pb–Pb	8.6 $\eta = 1$ Pb–Pb
$\gamma_q = 1$	T_{ch} [GeV]	0.212	0.263	0.280	0.304	0.324
	λ_q	4.14	2.36	1.49	1.56	1.61
	n_g/B	0.56	1.08	2.50	2.24	2.08
$\gamma_g = 1$	n_q/B	3.11	3.51	5.16	4.81	4.62
	$n_{\bar{q}}/B$	0.11	0.51	2.16	1.81	1.62
	$n_{\bar{s}}/B$	0.05	0.11	0.25	0.22	0.21
$\gamma_s = 0.15$	P_{ch} [GeV/fm ³]	0.46	0.76	0.79	1.12	1.46
	ρ_B	3.35	3.31	1.80	2.45	3.19
	S/B	12.3	19.7	41.8	37.4	34.9
$\gamma_q = 1$	γ_s	1	1	0.8	1	1
	T_0 [GeV]	0.184	0.215	0.233	0.239	0.255
$\gamma_g = 1$	λ_q	4.14	2.36	1.49	1.56	1.61
	$n_{\bar{s}}/B$	0.34	0.68	1.27	1.43	1.33
$\gamma_s = 0.8$ or	P_0 [GeV/fm ³]	0.30	0.41	0.47	0.54	0.71
	ρ_B	2.17	1.80	1.05	1.19	1.56
$\gamma_s = 1$	S/B	14.5	24.0	49.5	46.5	43.4

interesting properties (number of gluons per baryon, number of light quarks and antiquarks per baryon, number of anti-strange quarks per baryon, the pressure in the fireball, baryon density and the entropy per baryon) of the fireball.

At the end of QGP evolution, $t_0 \leq 5$ fm/c the strange quarks are near to absolute chemical equilibrium abundance and the temperature dropped from T_{ch} to the value T_0 as shown in the bottom portion of the table 1: full chemical equilibrium ($\gamma_s = 1$) is here assumed (with exception of the S–W case for which experimental results imply $\gamma_s = 0.8$ [11]). During the formation of the strangeness flavor we allow for fireball evolution, keeping the entropy content of gluons and light quarks constant. Conversion of energy into strangeness lowers the value of temperature to T_0 shown in table. This temperature is obtained as if the concurrent expansion cooling did not occur.

The temperature T_0 is closely related to the observed inverse slope T_{\perp} of the transverse mass spectrum fitted using the thermal spectral form $dN/m_{\perp}^{3/2} dm_{\perp} \propto \exp(-m_{\perp}/T_{\perp})$. Namely, the presence of some transparency (longitudinal flow) causes the central rapidity region $\Delta y = 1$ to feature in the m_{\perp} spectra the thermal shape normally seen after a sum over full rapidity range, here $\Delta y = 3$. Furthermore, we have in transverse direction either directly the emission of particles and hence $T_{\perp} \simeq T_0$, or there is collective radial flow in the QGP-hot matter, in which fraction of the thermal energy is converted into the flow energy. When

the final state particles emerge from the expanding volume and without re-equilibration, their spectral shape comprises the QGP temperature, blue-shifted by the flow velocity. This Doppler shift effect restores the freeze-out temperature to the high initial values[14], while absence of re-equilibration eliminates the reheating or cooling effects. For the S–W/Pb collisions at 8.8 GeV we have $T_0 = 233$ MeV, which result agrees very well with the experimental value $T_\perp = 232 \pm 5$ [6]. Similarly $\lambda_q = 1.49$ is in agreement with the results of our previous data analysis [11]. This agreement is a consequence of the choice $\alpha_s = 0.6$ in the QGP-EoS and stopping $\eta = 1/2$.

In Fig. 1 we show, as function of the specific energy content E/B , the behavior of temperature T_0 , the light quark fugacity λ_q and entropy per baryon S/B at full chemical equilibrium in the QGP fireball. The range of the possible values as function of η is indicated by showing results, for $\eta = 1$ (solid line), $1/2$ (dot-dashed line) and $1/4$ (dashed line). We note that, in qualitative terms, the drop in temperature with decreasing energy and stopping is intuitively as expected, and the value of λ_q is relatively insensitive to the stopping power. We note the (rapid) rise of specific entropy with E/B which should lead to a noticeable excess in the final particle abundances at CERN-SPS energies [15].

The experimental bars show for high (8.8 GeV) energy the result of WA85 data analysis [11], and for low energy (2.6 GeV) are taken from the analysis of the BNL-AGS data [16]. Note that in this case we had found $\lambda_s = 1.7$ and not $\lambda_s = 1$ as would be needed for the QGP interpretation at this low energy: Aside of the light quark fugacity there is also the strange quark fugacity not shown in Fig. 1, since in a strangeness neutral QGP fireball $\lambda_s = 1$, independent of the prevailing temperature and baryon density. This happens in general when both s and \bar{s} quarks have the same phase-space size, which is the case e.g. when they exist unbound. On the other hand, in confined forms of hadronic matter at finite baryon density there is a strong constraint between the two fugacities λ_q , and λ_s arising from the requirement of strangeness conservation [11]. These non-trivial relations between the parameters characterizing the final state particle abundances [1, 11] are in general difficult to satisfy, and thus lead to particle abundances which differ considerably between different final states. It is of importance to note that the two different collision systems analyzed at 200A GeV (S–W and S–S) [3, 6] lead to [11] $\lambda_s \simeq 1$ at different T_\perp . Our explanation of this result is that the particle source is a rapidly dissociating, deconfined fireball.

We now explore as function of energy the production of (strange) baryons and antibaryons. The ratios of (strange) antibaryons to strange baryons *of same particle type*: $R_N = \bar{p}/p$, $R_\Lambda = \bar{\Lambda}/\Lambda$, $R_\Xi = \bar{\Xi}/\Xi$ and $R_\Omega = \bar{\Omega}/\Omega$, are [1, 11] simple functions of the quark fugacities. The behavior of these ratios is shown in Fig. 2a as function of energy. It is obtained using the results for λ_q shown in Fig. 1, and taking the QGP value $\lambda_s = 1$. We have to remember that $R_\Omega = \lambda_s^{-6} = 1$, but since some re-equilibration is to be expected towards the HG behavior $\lambda_s > 1$, we expect $\lambda_s = 1 + \epsilon$, with ϵ small, and thus for this ratio $R_\Omega = 1 - 6\epsilon < 1$. A further non negligible correction which has been discussed in Ref. [11] is due to the isospin asymmetry.

In order to assess, as function of collision energy, the magnitude of the strange antibaryon yields per particle multiplicity formed in the collision, we need to establish the excitation function of the individual particle (antibaryon) yields. Considerable uncertainty is arising from the off-equilibrium nature of the hadronisation process, which in particular makes it

hard to estimate how the different heavy particle resonances are populated. Some of these uncertainties are eliminated when we normalize the yields in Fig. 2b at an energy, which we take here to be the value $E/B = 2.6$ GeV (we assume freeze-out temperature $T = 150$ MeV, $\gamma_s = 1$, $\eta_p = 1/2$ and absence of any re-equilibration after particle production). These yields increase with energy, as would be also expected in cascading hadron interactions, but contrary to such a picture in our approach the rise of more strange antibaryon yield is less pronounced.

We finally consider in Fig. 3 the particle ratios involving particles with differing strangeness content, and which are thus sensitive to the strangeness equilibration. The error bars show the key experimental results obtained at $\sqrt{s} = 8.6A$ GeV, compared to our theoretical results obtained with same phase space cuts on the range of p_\perp as in the experiments and presented here as function of energy. The $\bar{\Lambda}/\bar{p} \simeq 0.8 \pm 0.25$ ratio of the NA35 collaboration [17] was obtained for the S–Au system at 200A GeV for full phase space; WA85 precise value $\bar{\Xi}^-/\bar{\Lambda} = 0.21 \pm 0.02$ for $p_\perp > 1.2$ GeV, which result determines our choice $\gamma_s = 0.70$ and to a lesser degree also $\eta_p = 1/2$; and WA85 [7] $(\Omega + \bar{\Omega})/(\Xi^- + \bar{\Xi}^-) = 0.8 \pm 0.4$ for $p_\perp > 1.6$ GeV. The fact that the two ratio $\bar{\Lambda}/\bar{p}$ (NA35) and $(\Omega + \bar{\Omega})/(\Xi^- + \bar{\Xi}^-)$ (WA85) are satisfactorily explained, provides a very nice confirmation of the consistency of the thermal fireball model. We also draw attention to the remarkable behavior of the $\bar{\Xi}^-/\bar{\Lambda}$ ratio, which rises rapidly as the energy decreases.

The large $\bar{\Xi}^-/\bar{\Lambda}$ ratios in our QGP-fireball reaction picture are found even at relatively small energies, as is seen in Fig. 3. This is in contrast to microscopic models — near to $\bar{\Xi}^-$ production threshold in p – p interaction this ratio is exceedingly small. This lets us expect that as the energy rises towards the QGP formation threshold, there ought to be a considerable discontinuity in the relative $\bar{\Xi}^-/\bar{\Lambda}$ yield as function of collision energy. This provides for an interesting possibility to identify the energy at which collective QGP based production of strange antibaryons is first encountered.

At this threshold energy we should observe the onset of the other specific features of the deconfined hadronic phase: strange phase space saturation ($\gamma_s \rightarrow 1$), the associated strange particle production enhancement, pattern of strange antibaryon flow showing $\lambda_s = 1$, and entropy enhancement (particle multiplicity enhancement). If these features are indeed found, we can safely conclude that we have discovered a novel hadronic phase comprising deconfinement of s and \bar{s} quarks, rapid strangeness production, collective hadron production, high entropy content, as is expected of a rapidly dissociating quark-gluon plasma fireball.

Acknowledgment

J.R. acknowledges partial support by DOE, grant DE-FG03-95ER40937 .

References

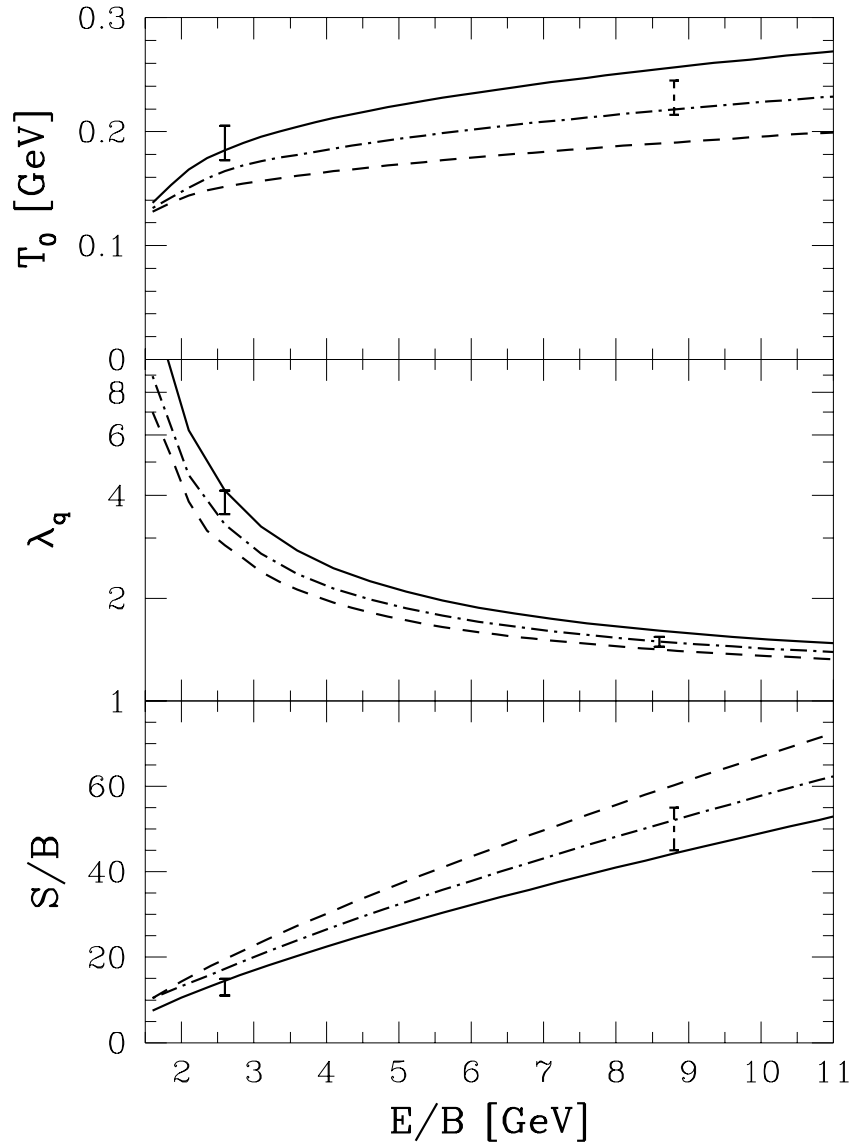
- [1] J. Rafelski, Phys. Lett. B **262**, 333 (1991); Nucl. Phys. A **544**, 279c (1992).
- [2] L. P. Csernai and I. N. Mishustin, Phys. Rev. Lett. **74**, 5005 (1995).

- [3] T. Alber et al. (NA35 collab.) *Z. Phys. C* **64**, 195 (1994).
- [4] J.D. Bjorken, *Phys. Rev. D* **27**, 140 (1983).
- [5] J. Rafelski and R. Hagedorn, *Statistical Mechanics of Quarks and Hadrons*, North-Holland, Amsterdam 1981, p. 253, edited by H. Satz ; J. Rafelski, *Phys. Rep. C* **88**, 331 (1982).
- [6] S. Abatzis et al. (WA94 collab.) *Phys. Lett. B* **354**, 178 (1995); D. Evans et al. (WA85 collab.), *Nucl. Phys. A* **566**, 225c (1994).
- [7] S. Abatzis et al. (WA85 collab.), *Phys. Lett. B* **347**, 158 (1995); *Phys. Lett. B* **316**, 615 (1993).
- [8] J. Rafelski and M. Danos, *Phys. Lett. B* **192**, 432 (1987); *Phys. Rev. D* **27**, 671 (1983).
- [9] J. Rafelski and B. Müller, *Phys. Rev. Lett.* **48**, 1066 (1982); **56**, 2334E (1986).
- [10] N. Bilić, J. Cleymans, I. Dadić and D. Hislop, *Phys. Rev. C* **53?**, . . . (1995) and references therein.
- [11] J. Letessier, A. Tounsi, U. Heinz, J. Sollfrank and J. Rafelski, *Phys. Rev. D* **51**, 3408 (1995); J. Sollfrank, M. Gaździcki, U. Heinz and J. Rafelski, *Z. Physik C* **61**, (1994); J. Letessier, J. Rafelski and A. Tounsi, *Phys. Lett. B* **321**, 394 (1994).
- [12] J. Letessier, J. Rafelski and A. Tounsi, *Phys. Lett. B* **323**, 393 (1994).
- [13] J. Letessier, J. Rafelski and A. Tounsi, *Phys. Lett. B* **333**, 484 (1994).
- [14] E. Schnedermann, J. Sollfrank and U. Heinz, *Particle Production in Highly Excited Matter*, NATO Physics series Vol. B **303**, Plenum Press, New York, 1993, p. 175, edited by H.H. Gutbrod and J. Rafelski.
- [15] J. Rafelski, J. Letessier and A. Tounsi, *XXVI International Conference on High Energy Physics*, Dallas, Texas, 1992, AIP-Conference Proceedings No 272, p. 983, edited by J.R. Sanford; J. Letessier, A. Tounsi, U. Heinz, J. Sollfrank and J. Rafelski, *Phys. Rev. Lett.* **70**, 3530 (1993); M. Gaździcki, *Z. Phys. C* **66**, 659, (1995).
- [16] J. Rafelski and M. Danos *Phys. Rev., C* **50**, 1684 (1994); J. Letessier, J. Rafelski and A. Tounsi, *Phys. Lett. B* **328**, 499 (1994); P. Braun-Munzinger and J. Stachel, in *Hot Hadronic Matter*, p451, NATO-ASI Series B: Physics Vol. 346, Plenum Press, New York 1995, edited by J. Letessier, H.H. Gutbrod and J. Rafelski.
- [17] T. Alber et al. (NA35 collab.), preprint IKF-HENPG/5-95, submitted to *Phys. Lett. B*; J. Günther et al. (NA35 collab.), to appear in proceedings of QM'95, Monterey, January 1995, edited by A. Poskanzer et al..

Figure 1: Temperature T_0 , light quark fugacity λ_q and entropy per baryon S/B at the time $t_0 \simeq 5 \text{ fm}/c$ of absolute chemical equilibration, as function of the QGP-fireball energy content E/B ; stopping $\eta = 1$ (solid line), $1/2$ (dot-dashed line) and $1/4$ (dashed line). See text for comparison with analysis results.

Figure 2: **a)** Antibaryon to baryon abundance ratios as function of energy per baryon E/B : $R_N = \bar{p}/p$ (solid line), $R_\Lambda = \bar{\Lambda}/\Lambda$ (long-dashed line), $R_\Xi = \bar{\Xi}/\Xi$ (short-dashed line) and $R_\Omega = \bar{\Omega}/\Omega$ (dotted line). **b)** Relative antibaryon yields as function of E/B : \bar{p} (solid line), $\bar{\Lambda}$ (long-dashed line), $\bar{\Xi}^-$ (short-dashed line) and $\bar{\Omega}$ (dotted line), all normalized to their respective yields at $E/B = 2.6 \text{ GeV}$.

Figure 3: Strange antibaryon ratios for S-W/Pb collisions as function of E/B : $\bar{\Lambda}/\bar{p}$ (full phase space), $\bar{\Xi}^-/\bar{\Lambda}$ for $p_\perp > 1.2 \text{ GeV}$ and $(\bar{\Omega} + \Omega)/(\bar{\Xi}^- + \Xi^-)$ for $p_\perp > 1.6 \text{ GeV}$; experimental results shown are from experiments NA35, WA85, see text for details.

**FIGURE 1**

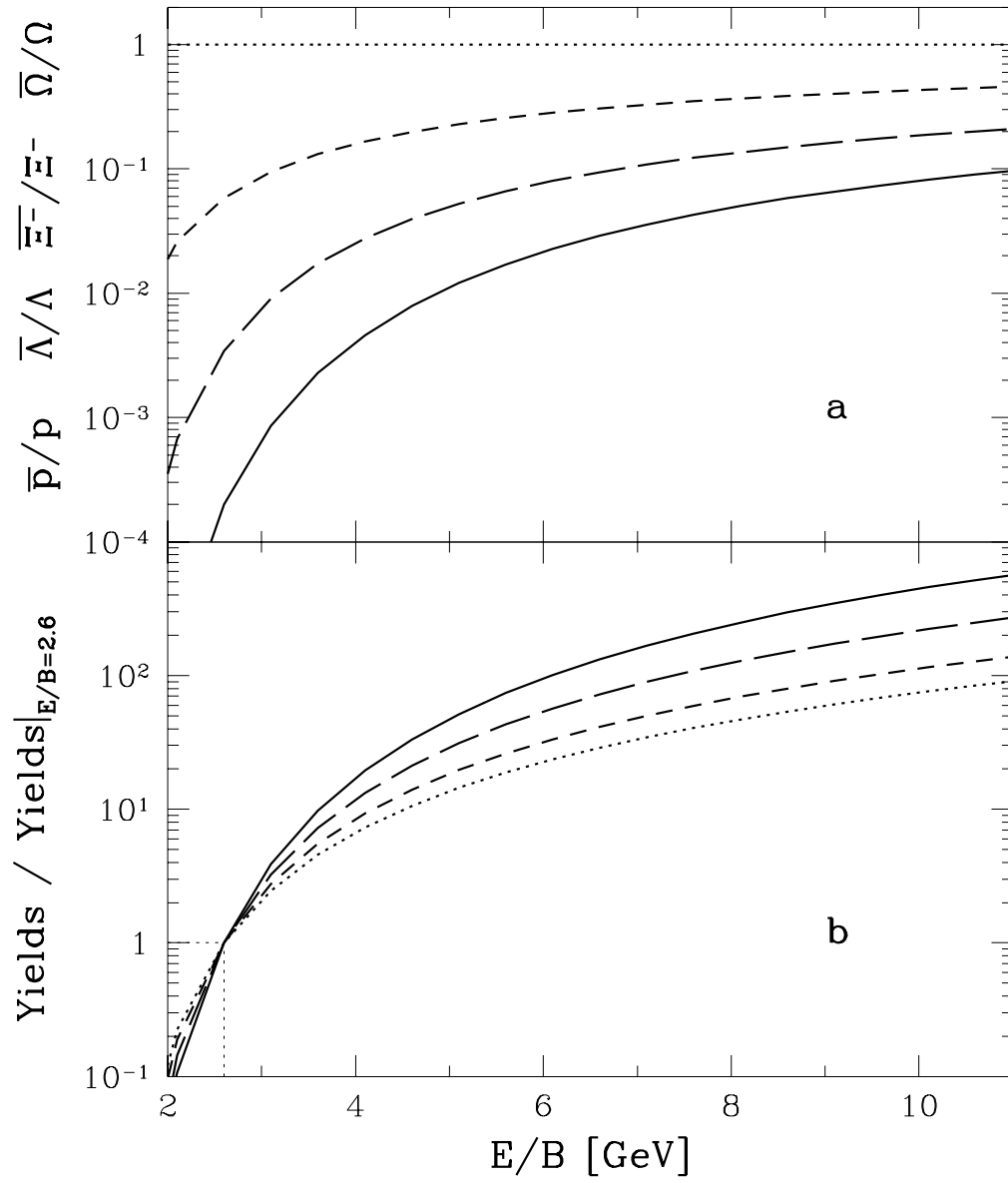
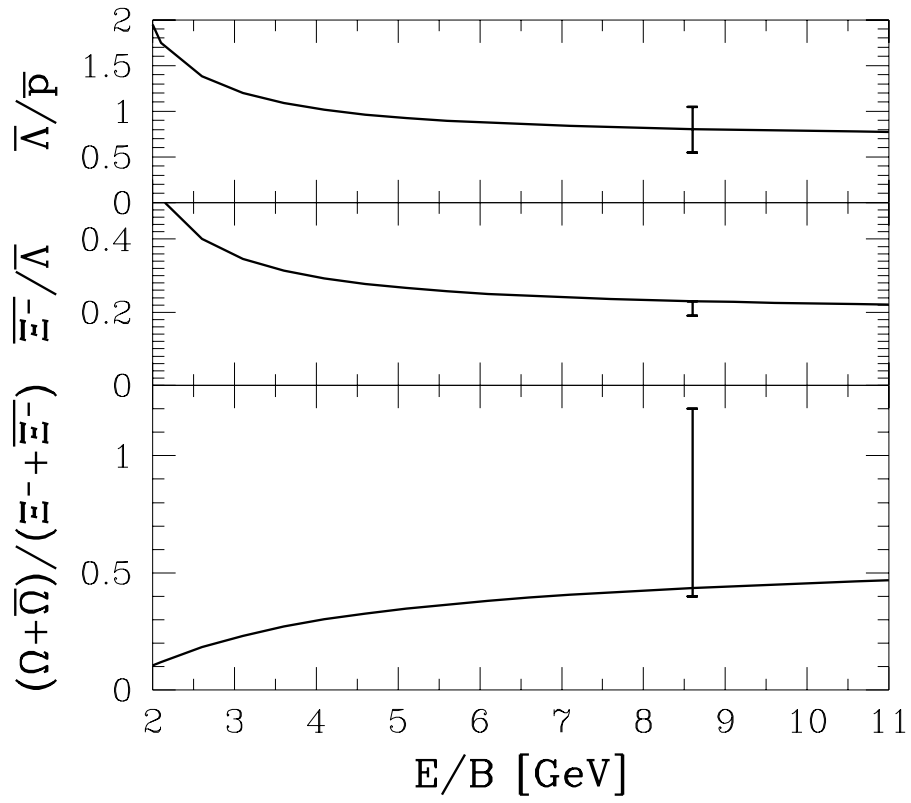


FIGURE 2

**FIGURE 3**